

X-ray Reflectivity Study of Thermal Capillary Waves on Liquid Surfaces

B. M. Ocko,¹ X. Z. Wu,² E. B. Sirota,² S. K. Sinha,² and M. Deutsch³

¹*Physics Department, Brookhaven National Laboratory, Upton, New York 11973*

²*Corporate Research Laboratory, Exxon Research and Engineering Company, Route 22 East, Annandale, New Jersey 08801*

³*Physics Department, Bar Ilan University, Ramat Gan 52900, Israel*

(Received 8 October 1993)

X-ray reflectivity measurements have been carried out at the liquid/vapor interface of normal alkanes. The reflectivities over a large temperature range of different chain lengths (C20 and C36) provide a critical test of the various capillary wave models. Our data are most consistent with the hybrid model which allows for a molecular size dependent cutoff q_{\max} for the capillary waves and an intrinsic interface width σ_0 .

PACS numbers: 68.10.-m, 61.25.Em, 64.70.Dv

It has long been realized that the density variation normal to the liquid free surface is gradual and continuous. However, the exact origins, shape, temperature dependence, etc., of this profile are still not fully understood. The mean-field theory of van der Waals [1] and its modern extensions by Widom and co-workers [2] predict a smooth, continuous compositional profile whose width depends on the bulk correlation length only. The continuous nature of the interface was first ascribed to thermally excited capillary waves by Buff, Lovett, and Stillinger (BLS) [3], who extended the macroscopic elasticity theory to microscopic lengths. They calculated the interfacial width by integrating the thermally excited capillary spectrum from the long-wavelength gravitational cutoff, $q_{\min} \approx 1 \text{ cm}^{-1}$, to a short-wavelength cutoff, $q_{\max} \approx \pi/a$, determined by the molecular size a . The BLS model has been further refined by the inclusion of an intrinsic profile of finite width [4], the renormalization of the surface tension [5], the introduction of coupling between the capillary modes [6], etc. However, the physical origin for q_{\max} and the intrinsic interfacial width σ_0 are not universal for these theories [7].

Close to criticality, the widths of the liquid-vapor interface ranges from hundreds to thousands of Å. Within this region, optical ellipsometry and reflectometry experiments [8–10] have been employed extensively to study the liquid-vapor interface. However, far from criticality the widths have been measured [6, 8] to be less than 10 Å and these optical techniques do not provide sufficient resolution to test the different theoretical approaches. Since x-ray surface techniques provide sub-Å resolution [11–14], they are well suited to study the noncritical liquid-vapor interface profile. Specular reflectivity has been used to measure the mean capillary wave amplitudes [13–16], whereas the diffuse scattering has provided information on the in-plane correlations [14, 15, 17]. These studies demonstrate that the capillary wave spectrum can be probed up to the long-wavelength limit imposed by the x-ray instrumental resolution. Since all of these previous studies were carried out with liquids of similar molecular size and at room temperature only, the magnitude and physical origins of q_{\max} remain controversial. In the

present work, we employ x-ray reflectivity to study the density profile of the free surface of liquid alkanes with different molecular sizes over a large temperature range. Our results, which are described best by the hybrid capillary model, yield an intrinsic width of $\sigma_0 \approx 1 \text{ Å}$ for the interface, and a short-wavelength cutoff q_{\max} related to the molecular size. Both parameters are found to be temperature independent.

In an x-ray reflectivity measurement, a beam of wavelength λ is incident upon a horizontal liquid surface at a grazing angle α , and a detector is placed at an angle $\beta = \alpha$ in the plane of reflection to measure the reflected intensity. In this configuration, the wave-vector transfer $q_z = (4\pi/\lambda) \sin(\alpha)$ is normal to the liquid surface, thus the reflectivity probes the electron density profile along that direction. For an ideally smooth and sharp interface, the reflectivity $R(q_z)$ is purely specular and is given by the Fresnel reflectivity $R_F(q_z)$, shown in Fig. 1. For an actual liquid interface, the reflectivity is no longer purely specular, as the diffuse scattering from the capillary fluctuations also contributes to the measured intensity [13, 14]. To a very good approximation, the reflectivity is only modified by a Debye-Waller-like factor [13, 18] and is given by

$$R(q_z) = R_F(q_z) \exp(-q_z^2 \sigma_{\text{eff}}^2), \quad (1)$$

where σ_{eff} is the effective width of the liquid interface and is discussed below. Thus, a fit of Eq. (1) by the measured x-ray reflectivity of a given liquid surface allows, in principle, the determination of the interfacial width.

Following the reviews by Gelfand and Fisher [7] and Beysens and Robert [19], all capillary wave theories result in the following expression for the width σ of the liquid-vapor interface:

$$\sigma^2 = \sigma_0^2 + \sigma_{\text{cw}}^2 = \sigma_0^2 + \frac{k_b T}{2\pi\gamma_{\text{cw}}} \ln\left(\frac{q_{\max}}{q_{\min}}\right). \quad (2)$$

where σ_0 and σ_{cw} are the intrinsic and capillary contributions to the surface width, respectively. q_{\max} is the short-wavelength cutoff which must be smaller than π/a where a is the molecular size. The origin and exact nature of σ_0 and q_{\max} are model dependent. Gravity imposes a

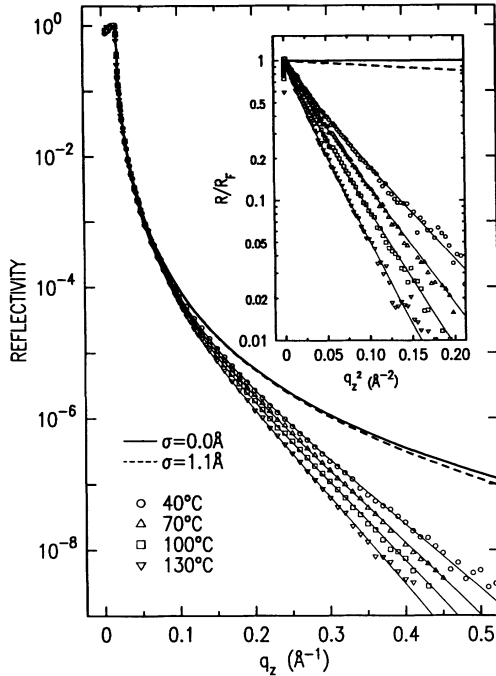


FIG. 1. X-ray reflectivities of C20 at $T = 40, 70, 100$, and 130°C (open symbols). Note the increase with temperature in the rate of decrease with q_z . The lines through the symbols are the fits discussed in the text. The solid line is the Fresnel reflectivity R_F and the dotted line is the reflectivity with an interface width $\sigma_0 = 1.1 \text{ \AA}$. In the inset, the reflectivities normalized by the R_F are plotted as a function of q_z^2 .

long-wavelength cutoff [7], $q_{\min} = q_g = \sqrt{\Delta\rho g/\gamma_{\text{cw}}}$ with g the gravitational acceleration, γ_{cw} the surface tension associated with the capillary waves, and $\Delta\rho$ the mass density difference between the liquid and its vapor.

In reflectivity measurements, the longest coherence length $4\pi/q_z\Delta\beta$ that can be resolved by the instrument is always much smaller than $2\pi/q_g$ [13], where $\Delta\beta$ is the angular acceptance of the detector in the plane of reflection. This results in $q_{\min} = q_z\Delta\beta/2$ for the configuration used in our experiment, and consequently the effective interface width measured with x-ray reflectivity is given by [20]

$$\sigma_{\text{eff}}^2 = \sigma_0^2 + \frac{kT}{2\pi\gamma} \ln\left(\frac{2q_{\max}}{q_z\Delta\beta}\right). \quad (3)$$

Note the q_z dependence of this expression, which is often unjustly neglected in the determination of surface "roughness" by x-ray methods. The resolution dependence of the second term has been experimentally verified by Braslau *et al.* [13]. Although the second term is significantly smaller than that obtained when using the gravitational cutoff [7], it is still much larger than σ_0^2 .

The x-ray reflectivity measurements were done at beam line X22B of the National Synchrotron Light Source using the Harvard-BNL liquid spectrometer at $\lambda = 1.53 \text{ \AA}$ and with an angular resolution of $\Delta\beta = 3.3$

mrad. The samples, normal alkanes $\text{CH}_3\text{-(CH}_2\text{)}_{n-2}\text{-CH}_3$ (denoted C $_n$) have nominal purities $\geq 99\%$. Each sample consisted of a puddle $\sim 70 \text{ mm}$ in diameter and $\sim 0.5 \text{ mm}$ thick, contained in a sealed beryllium cell, the temperature of which was regulated to $\leq 5 \times 10^{-3}^\circ\text{C}$ [21]. No x-ray exposure effects or temperature-cycling degradation effects were observed. Previously it has been shown that a crystalline monomolecular layer forms at the surface of liquid alkanes at temperatures of up to 3°C above their bulk freezing temperatures [21]. In the present study reflectivity spectra were obtained for C20 at eleven temperatures in the range $40^\circ\text{C} < T < 140^\circ\text{C}$ and for C36 at four temperatures in the range $80^\circ\text{C} < T < 140^\circ\text{C}$. These temperatures are well above the surface crystallization temperature.

The measured reflectivities of C20 at $T = 40, 70, 100$, and 130°C are shown in Fig. 1. Their overall q_z dependence is typical of reflectivities measured for simple liquid surfaces such as water and ethanol [13, 14]. Furthermore, it is clearly observed that the rate of decrease of the reflectivity with q_z is higher at higher temperatures, as expected from Eqs. (1) and (3). To fit these data with Eq. (3), we measured the surface tension of C20 and C36 using the Wilhelmy plate method [22] over the same temperature range as the x-ray measurements. The cell is similar to the one used for x-ray measurements except for a hole in the top for the wire holding the plate. As the vapor pressures of both compounds are negligible at these temperatures the closure of the cell is not important. The measured surface tensions γ , plotted in the inset of Fig. 3, are described by $\gamma_{\text{C20}} = 31.49 - 0.0848T$ dyn/cm, and $\gamma_{\text{C36}} = 35.30 - 0.0920T$ dyn/cm, with T in $^\circ\text{C}$. To calculate the gravitational long-wavelength cutoff, we used the literature values of the liquid density, given by $\rho_{\text{C20}} = 0.803 - 6.75 \times 10^{-4}T$ g/cm 3 [23], and $\rho_{\text{C36}} = 0.829 - 6.20 \times 10^{-4}T$ g/cm 3 [24]. The critical angles obtained from the reflectivity are in consistent agreement with the values calculated from these densities.

We have utilized the hybrid capillary wave model, proposed by Weeks [4], to fit the reflectivity data. This model has, in Eqs. (2) and (3), γ_{cw} equal to the macroscopic, measured surface tension γ and leaves q_{\max} as a free parameter, of the order of π/ξ , where ξ is the bulk correlation length. Fluctuations on wavelengths shorter than ξ are assumed to give rise to a finite intrinsic interfacial width σ_0 . Most previous x-ray reflectivity measurements at the liquid-vapor interface have utilized this formulation [13–15]. However, even though σ_{cw} is q_z dependent and σ_0 is q_z independent, the weak logarithmic q_z dependence is insufficient for separating these two terms in fitting reflectivity data measured at a single temperature. By measuring the data over a large temperature range the prospects of separating σ_{cw} from σ_0 are greatly enhanced. Here we assume that q_{\max} and σ_0 are determined by the molecular size, and thus are temperature independent and common to all measured reflectivities.

ity curves of a single compound. For C20, the reflectivity curves measured at eleven different temperature were fitted simultaneously by Eqs. (1) and (3). σ_0 and q_{\max} were found to be strongly coupled: the larger σ_0 , the smaller σ_{cw} and, consequently, q_{\max} [Fig. 2(a)]. A minimal χ^2 was achieved for $\sigma_0 = 1.1 \text{ \AA}$ and $q_{\max} = 0.44 \text{ \AA}^{-1}$ [Fig. 2(b)]. As demonstrated by Fig. 1, the model provides an excellent description of the data over the entire temperature range. The reflectivity curve (dashed line in Fig. 1), with $\sigma_0 = 1.1 \text{ \AA}$ for σ_{eff} , without the capillary wave contribution, demonstrates that the capillary wave term in Eq. (3) is dominant. The shallow minimum of χ^2 with respect to σ_0 [see Fig. 2(b)] is a direct consequence of the weak q_z dependence of the capillary term in Eq. (2) and the small contribution from σ_0 .

To further elucidate the behavior of q_{\max} , we set σ_0 equal to 1.1 \AA and fit the reflectivities at each temperature with a free q_{\max} . The resultant q_{\max} is effectively constant over the 100°C range and is equal to $0.44 \pm 0.06 \text{ \AA}^{-1}$. The absence of a systematic temperature dependence is consistent with our starting assumption that σ_0 and q_{\max} are related to the molecular size. The value of σ_0 is close to the carbon-carbon bond length a_0 of 1.5 \AA . The effective cutoff length, $\pi/q_{\max} \approx 7.1 \text{ \AA}$, is significantly larger than the corresponding length for simple liquids obtained previously. For instance, $\pi/q_{\max} \approx 1.9 \text{ \AA}$ for water, $\pi/q_{\max} \approx 2.5 \text{ \AA}$ for methanol, and $\pi/q_{\max} \approx 3.4 \text{ \AA}$ for carbon tetrachloride [13]. The radius of the alkane chain in the liquid state is between half the fully extended chain length, 12 \AA , and the radius of gyration of a randomly coiled chain, $\sqrt{2(N-1)/3}a_0 \approx 5.3 \text{ \AA}$. The 7.1 \AA cutoff obtained here is consistent with these values.

Similar fits were also carried out for the C36 data.

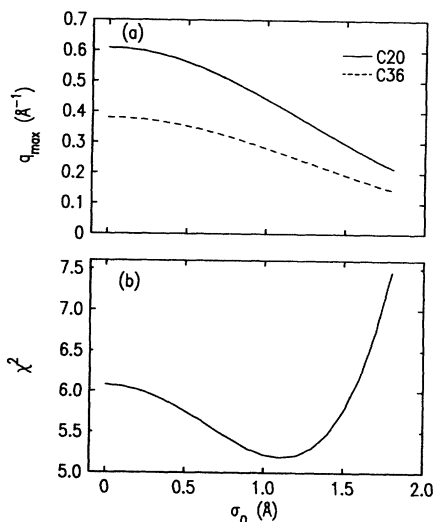


FIG. 2. (a) The variation of q_{\max} with σ_0 in the simultaneous fit of the measured eleven reflectivity curves for C20 (solid line) and of the four reflectivities measured for C36 (dotted line). (b) The χ^2 variation with σ_0 of the simultaneous fit of the eleven reflectivities for C20.

The limited temperature range between the C36 freezing temperature and 140°C results in a more shallow minimum in the χ^2 curve (not shown) than for C20. Based on the assumption that σ_0 is determined by the C-C bond length, we fixed σ_0 at the value obtained for C20 in order to make a direct comparison between both chain lengths. This procedure yields a temperature independent $q_{\max} = 0.27 \pm 0.03 \text{ \AA}^{-1}$, or a corresponding $\pi/q_{\max} = 11.6 \text{ \AA}$. The ratio of these lengths, $11.6/7.1 \approx 1.6 \pm 0.3$, lies between the carbon number ratio of C20 and C36, $36/20=1.8$, and its square root, 1.3, also in accordance with the interpretation of q_{\max} as a molecular size determined cutoff.

In Fig. 3 we show the temperature dependence of the interfacial width σ_{eff} , evaluated at $q_z = 0.4 \text{ \AA}^{-1}$, for C20 (circles) and C36 (squares) obtained by fitting the reflectivity profiles. The dashed lines were obtained from the capillary wave fits with a constant q_{\max} obtained by fitting reflectivities of all temperatures simultaneously, and the open circles and squares were obtained when q_{\max} was allowed to float at each temperature. The small scatter of the symbols relative to the dashed lines demonstrates the two parameter model is in good agreement with the experimental results. For C20 σ_{eff} increases from 4.2 \AA at 40°C to 5.5 \AA at 140°C . At all temperatures σ_{eff} for C20 is larger than for C36 due to its lower surface tension γ and higher q_{\max} . In Fig. 3, we also show the temperature dependence of the "true" σ which is obtained by integrating over all capillary modes from the gravitational cutoff up to q_{\max} . The solid lines are the values

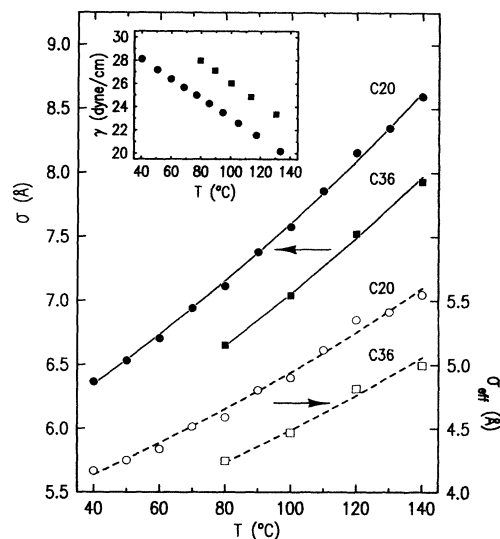


FIG. 3. The interface width σ and effective width σ_{eff} of C20 and C36 as a function of temperatures. Respectively, σ and σ_{eff} of C20 are in closed and open circles, σ and σ_{eff} of C36 are in closed and open squares. The lines are the corresponding widths calculated with $\sigma_0 = 1.1 \text{ \AA}$, $q_{\max} = 0.44 \text{ \AA}^{-1}$ for C20 and $q_{\max} = 0.27 \text{ \AA}^{-1}$ for C36. The inset shows the measured surface tension γ of C20 (circles) and C36 (squares).

obtained with a single q_{\max} for each compound, while the solid circles and squares are the values obtained with different q_{\max} at different temperatures. Unlike σ_{eff} , σ is the total interface width and is free from instrumental resolution effects. Since the finite instrumental resolution excludes a range of modes from the measurements, σ_{eff} is always smaller than σ . For example, for C20 at 40°C, $q_g = 5 \times 10^{-8} \text{ \AA}^{-1}$ yields a full capillary wavelength range from 7 Å to $6 \times 10^8 \text{ \AA}$. The finite resolution, however, decreases π/q_{\min} which reduces the maximum capillary wavelength to $\approx 5 \times 10^3 \text{ \AA}$ at $q_z = 0.4 \text{ \AA}^{-1}$.

We now discuss our measurements within the context of the BLS model [3]. This model assumes a sharp intrinsic interface, i.e., $\sigma_0 = 0$, with q_{\max} determined self-consistently by $q_{\max} = \pi/\sigma$ [see Eq. (2)]. Also, γ_{cw} is the surface tension of the "bare" interface, which is related to the macroscopic surface tension γ by $\gamma_{\text{cw}} = \gamma + (3k_b T/16\pi)q_{\max}^2$. The use of this γ_{cw} in Eqs. (1) and (3) yields an upper bound on σ and σ_{eff} for each temperature, which are about 1 Å too small to account for the observed decrease in the reflectivity with q_z . Thus it is impossible to fit the reflectivity data with the BLS capillary wave model. This is not very surprising since the continuum-matter BLS theory does not provide for the additional roughness due to the finite molecular size.

We have also checked the validity of the mode coupling capillary wave model [6] for our measured reflectivities. This model effectively reduces to Eqs. (1) and (3) with a temperature dependent cutoff $q_{\max}^{\text{MC}} = \sqrt{8\pi\gamma/3k_b T}$ which does not depend explicitly on the molecular size. Using the measured surface tension, we obtain for C20 $q_{\max}^{\text{MC}} = 0.72$ and 0.52 \AA^{-1} at 40 and 140°C, respectively. Likewise, for C36 $q_{\max}^{\text{MC}} = 0.63$ and 0.57 \AA^{-1} for 80 and 140°C. From Fig. 2(a) it is apparent that such a large q_{\max}^{MC} value requires $\sigma_0 = 0$ for C20 and results in a larger χ^2 in the fit than that of the hybrid model. For C36 the q_{\max}^{MC} value obtained even requires an imaginary value for σ_0 to fit the data, which is of course unphysical. All this indicates that the mode coupling model is less favored by the data than the hybrid model. However, the influence of mode coupling on the measured data is expected to be small in our case. The molecular size cutoffs q_{\max} are smaller here than the mode coupling ones, and will, therefore, be the ones limiting the spectrum in practice. The fact that previous liquid x-ray reflectivity spectra [16,19] could be described by the mode coupling theories with $q_{\max} = q_{\max}^{\text{MC}}$ may be serendipitous since for the small molecules of previous studies q_{\max}^{MC} coincides with the molecular size cutoff.

The temperature and molecular size dependent study of the surface of liquid normal alkanes, presented here, provides strong experimental support for the hybrid theory, which views the noncritical liquid-vapor interface as having an intrinsic width broadened further by thermally induced capillary waves, with wavelengths extending down to the molecular size. While the BLS theory is found to be clearly unsupportable, the cutoff given by the

mode coupling theory is not relevant in the present studies, even though it may be applicable to liquid surfaces of small molecular sizes. Further studies over larger temperature ranges and for smaller molecules are required to gain insight into this problem.

The work of M.D. is supported by the U.S.-Israel Binational Science Foundation, Jerusalem. Brookhaven National Laboratory is supported by the Division of Materials Research, U.S. Department of Energy under Contract No. DE-AC02-76CH00016.

- [1] J. D. van der Waals, *Z. Phys. Chem.* **13**, 657 (1894).
- [2] J. S. Rowlinson and B. Widom, *Molecular Theory of Capillarity* (Clarendon, Oxford, 1982); S. Fisk and B. Widom, *J. Chem. Phys.* **50**, 3119 (1969).
- [3] F. P. Buff, R. A. Lovett, and F. H. Stillinger, *Phys. Rev. Lett.* **15**, 621 (1965).
- [4] J. D. Weeks, *J. Chem. Phys.* **67**, 3106 (1977).
- [5] J. V. Sengers and J. M. J. van Leeuwen, *Phys. Rev. A* **39**, 6346 (1989).
- [6] J. Meunier, *J. Phys. (Paris)* **48**, 1819 (1987).
- [7] M. P. Gelfand and M. E. Fisher, *Physica (Amsterdam)* **166A**, 1 (1990).
- [8] D. Beaglehole, *Phys. Rev. Lett.* **58**, 1434 (1987).
- [9] E. S. Wu and W. W. Webb, *Phys. Rev. A* **8**, 2065 (1973).
- [10] J. W. Schmidt, *Physica (Amsterdam)* **172A**, 40 (1991); J. W. Schmidt and M. R. Moldover, *J. Chem. Phys.* **99**, 582 (1993).
- [11] J. Als-Nielsen, *Physica (Amsterdam)* **140A**, 376 (1986).
- [12] S. K. Sinha, E. B. Sirota, S. Garoff, and H. B. Stanley, *Phys. Rev. B* **38**, 2297 (1988).
- [13] A. Braslau, P. S. Pershan, and G. Swislow, *Phys. Rev. A* **38**, 2457 (1989); A. Braslau, M. Deutsch, P. S. Pershan, A. H. Weiss, J. Als-Nielsen, and J. Bohr, *Phys. Rev. Lett.* **54**, 114 (1985).
- [14] M. K. Sanyal, S. K. Sinha, K. G. Huang, and B. M. Ocko, *Phys. Rev. Lett.* **66**, 628 (1991).
- [15] D. K. Schwartz, M. L. Schlossman, E. H. Kawamoto, G. J. Kellogg, P. S. Pershan, and B. M. Ocko, *Phys. Rev. A* **41**, 5687 (1990).
- [16] J. Daillant, L. Bosio, J. J. Benattar, and J. Meunier, *Europhys. Lett.* **8**, 5 (1989).
- [17] W. Zhao, X. Zhao, J. Sokolov, M. H. Rafailovich, M. K. Sanyal, S. K. Sinha, B. H. Cao, M. W. Kim, and B. B. Sauer, *J. Chem. Phys.* **97**, 8536 (1992).
- [18] Using an approach similar to that of Ref. [14] an expression identical to that of Ref. [13] has been obtained by S. K. Sinha (to be published).
- [19] D. Beysens and M. Robert, *J. Chem. Phys.* **87**, 3056 (1987).
- [20] q_{\min} in Eq. (2) can be approximated by $q_z \Delta \beta / 2$ when the detector slits out of the detector plane are sufficiently wide open. This approximation has been checked numerically for our experimental configuration.
- [21] X. Z. Wu, E. B. Sirota, S. K. Sinha, B. M. Ocko, and M. Deutsch, *Phys. Rev. Lett.* **70**, 958 (1993).
- [22] G. L. Gaines, *Insoluble Monolayers at the Liquid Gas Interface* (Wiley, New York, 1966).
- [23] D. M. Small, *The Physical Chemistry of Lipids* (Plenum, New York, 1986).
- [24] *Properties of Hydrocarbons of High Molecular Weight*, API Research Project 42 (API, Washington, DC, 1966).